ELSEVIER

Ceramics International 28 (2002) 153–158

CERAMICS INTERNATIONAL

www.elsevier.com/locate/ceramint

Microstructural and mechanical properties of nanocrystalline spinel and related composites

S. Bhaduri, S.B. Bhaduri*

Department of Materials and Metallurgical Engineering, University of Idaho, Moscow, ID 83844-3024, USA

Received 3 May 2001; received in revised form 15 May 2001; accepted 25 June 2001

Abstract

Magnesium aluminate spinel ($MgAl_2O_4$) is known for its excellent deformation behavior at high temperatures. By retaining nanocrystalline grain size after densification, the extent of deformation can be further enhanced. In this work, nanocrystalline $MgAl_2O_4$ and composites were densified by hot isostatic pressing (HIPing). One of the objectives of this paper is to report the phase content and microstructural characteristics of these dense nanocomposites. Another objective is to investigate room temperature as well as high temperature mechanical properties of these materials. The present data were compared with the existing literature for coarse grained materials. The hardness values ranged between 2.89 and 7.79 GPa and fracture toughness ranged between 2.5 and 5.82 MPa$\sqrt{m}$. Hot hardness results showed that at least in one composition, a significant reduction in hardness occurred at 1000 °C.

Keywords: B. Microstructure; C. Mechanical properties; Spinel composites

1. Introduction

It is has been argued that, by decreasing grain size, traditionally ductile metals can be made hard, strong and brittle [1]. On the other hand, nanocrystalline ceramics can deform plastically because of possible creep diffusion and grain boundary sliding [1]. Ceramic nanocomposites are expected to have further advantages over the single phase materials. An overview of processing and consolidation of ceramic nanocomposites was presented by the present authors [2]. Briefly, ceramic nanocomposites are divided into four classes: inter, intra, hybrid and nano/nano. Nano/nano composites are believed to undergo enhanced creep which is helpful in superplastic deformation [3]. On the other hand, intragranular and intra type composites show 2–5 times the toughness and strength at room temperature than those of single phase materials [3].

Mechanical behavior of spinels at room as well as high temperatures has been reported in the literature. Stewart and Bradt [4] reported temperature dependent fracture toughness of spinel for different grain sizes. Ghosh et al. [5] reported fracture toughness of spinels from room temperature to 1400 °C. Room temperature toughness and R-curve behavior are available in several references [6–8]. These papers do not mention how the toughness would change if nanocrystalline grain sizes were maintained after densification. A high temperature mechanical property, such as creep behavior, was reported by Corman [9], Beclin et al. [10] and Lappalainen et al. [11] for stoichiometric as well as off stoichiometric spinels. Also, superplastic deformation experiments were performed by different authors [12–16]. In general, it was found that a spinel is deformable at moderate temperatures. Therefore, it is expected that the extent of deformation would increase and occur at lower temperatures if the nanocrystalline grain size was maintained.

The present authors reported the synthesis of in situ mixed nanocomposites by an auto-ignition process [17]. This paper is the sequel to the earlier work and reports the densification of the powders by hot isostatic pressing. The phase content and microstructural characteristics are examined. The room temperature as well as high temperature mechanical properties of dense nanocrystalline $MgAl_2O_4$ and its related composites are also determined.

* Corresponding author. Tel.: +1-208-885-6376; fax: +1-208-885-2855.

E-mail address: bhaduri@uidaho.edu (S.B. Bhaduri).

0272-8842/02/$22.00
PII: S0272-8842(01)00071-2

2. Experimental procedure

2.1. Consolidation of powders

The powders used for the consolidation were synthesized by auto-ignition processing [17]. A total of four nominal compositions were chosen for densification (A: Al_2O_3–14 mol% MgO, B: Al_2O_3–20 mol% MgO, C: Al_2O_3–40 mol% MgO and D: Al_2O_3–50 mol% MgO). They were chosen based on heat-treatment studies [18]. For example, some compositions showed grain growth at 1200 °C when heat treated for 2 h [18]. These compositions were not suitable for further densification studies because the purpose of the study was to attain full density without losing nanocrystallinity.

It was found that the as-synthesized powders were loosely agglomerated. In order to break up the agglomerates and improve the homogeneity of the powders, a slip casting method was adopted. The powders were crushed lightly and placed in a glass bottle with Al_2O_3 balls (supplied by Coors, Colorado, Co) approximately 1:5 ratio. Deionized water mixed with dilute nitric acid was used as a dispersing medium. The pH of the liquid was carefully controlled so that pH was in the 2.5–3 range. The slurries were subsequently ball milled for 3–4 h A mold was made up of gypsum and water with a 70:100 ratio. This suspension was selected for casting because it resulted in a more controlled wall thickness formation. The slurry was directly poured into the mold. After drying, the powders seemed to flow freely and were pressed at 70 MPa level pressure using a hardened steel die of approximately 0.51 inches diameter in a uniaxial press. Approximately two green compacts were made from each composition. The pellets were cold isostatically pressed (CIPed) (Isospectrum, Columbus, OH) at a pressure of 275 MPa, maintained for 10 min.

After CIPing, the samples were encapsulated in a pyrex glass tube of diameter 15mm and sealed at one end. In order to prevent the interaction of the glass and the samples, BN spray was used. The tubes were subsequently necked about 2 in from the bottom. The evacuation of a tube continued until a vacuum level of 10^{-3} Torr was reached and was sealed at the neck using an oxygen–methane torch. The encapsulated samples were placed in a graphite crucible placed in a hot zone of a HIP (Isospectrum, Columbus, OH). The HIP is capable of a maximum pressure of 207 MPa (30 ksi) and a maximum temperature of 2000 °C. The pressure vessel was evacuated and backfilled at least twice with Ar. The furnace was programmed to rise to an appropriate temperature while the holding time was 2–4 h, depending on the composition, at a pressure of 179 MPa. Pressure was applied approximately at 800 °C when the glass began to soften. The sample was cooled down slowly to minimize the thermal gradient that generally induces microcracking. Finally, the glass tube was broken to remove the specimen.

2.2. Compact characterization

After HIPing, the samples were mounted and polished with 9, 6, 3, 1 and 0.5 μm diamond polish to a mirror finish. For grain size and grain structure determination, the samples were thermally etched in a furnace at 1100 °C for 0.5 h. The microstructures of the as-polished and as-etched samples were examined by a scanning electron microscope (SEM model (AMRAY 1830) equipped with an energy dispersive X-ray analyzer. The phases and grain sizes of the samples were analyzed by X-ray diffraction patterns of the product and were recorded by a Siemens diffractometer (D5000) using CuK_α radiation at 40 kV and 30 mA.

2.3. Mechanical property testing

The samples were tested for hardness and fracture toughness by an indentation fracture technique using different load values. Vickers hardness testers were used for indentation (Zwick hardness tester: model 3212 and Leco M-400-G). Room temperature hardness data were measured on at least ten distinct areas of the sample. In some compositions, 10 kg of load was tried, but chipping around the indentation impaired accurate measurements. One and 5 kg loads were used. For the fracture toughness measurement, the equation derived by Evans and Charles [19] and the one proposed by Niihara et al. [20] were used. In the first case, crack length is small compared with the dimension of the Vickers indent and, in the latter, the crack length is larger or equal to the that of the indent.

Hot hardness was measured using a Nikon QM-1 hot hardness indenter with a diamond pyramid indenter. The samples were mounted on a molybdenum holder. The temperatures of the indenter and the specimen were controlled separately. All tests were performed in vacuum up to 10^{-5} Torr or better. A 500 g load was used for 10 s with a minimum of 5 repetitions per test. Indentations were examined at 400 times magnification that gave direct readings in microns.

3. Results and discussions

3.1. Phase and microstructural characterization

Fig. 1 shows the X-ray diffraction patterns of samples HIPed at 1200–1300 °C for 2–4 h. In compositions A and B, two phases were identified: α-Al_2O_3 and $MgAl_2O_4$. Due to the high temperature exposure, some grain growth had occurred and was evident in the sharpening of diffraction lines. In composition A, the intensity of α-Al_2O_3 and $MgAl_2O_4$ were almost 50–50. In composition B, the intensity of $MgAl_2O_4$ increased as expected because of more MgO content. For compositions C and

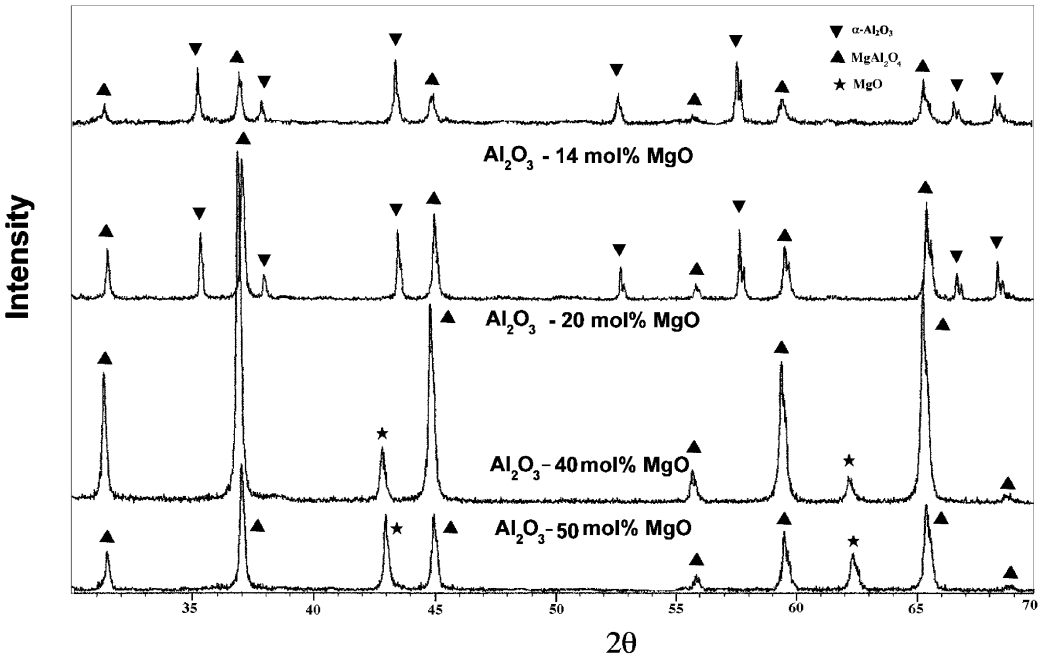

Fig. 1. X-ray diffraction patterns of the sample HIPed at 1200–1300 °C for 2–4 h. 1: Composition D (Al_2O_3–50 mol% MgO for 1300 °C, 2 h); 2: Composition C (Al_2O_3–40 mol% MgO for 1200 °C, 2 h); 3: composition B (Al_2O_3–20 mol% MgO for 1300 °C, 2 h); 4: composition A (Al_2O_3–14 mol% MgO for 1200 °C, 2 h).

D, the presence of $MgAl_2O_4$ and MgO was identified. For these two compositions, no trace of α-Al_2O_3 was found in the X-ray data. Sharpening of the diffraction lines was also evidenced in the X-ray diffraction pattern. In composition D, the intensity of MgO content increased as expected.

The microstructures of as-HIPed materials were characterized using scanning electron microscopy. Fig. 2 shows a SEM micrograph of as-HIPed sample of composition B, HIPed at 1300 °C for 2 h. The grain sizes were in the 100–150 nm range. The entire sample was dense. This composition took longer to densify compared to composition A, which densified at a lower temperature. Grains were equiaxed in nature. This kind of equiaxed grain microstructure is ideal for superplastic deformation. Fig. 3 is a micrograph of a crack generated by the indentation of a load of 5 kg for composition (described in section B). Note that cracks emanate from the corners of the indents and crack lengths were fairly large compared to the Vickers hardness impression, showing brittleness of the material. This was the only case where crack length was large compared with the Vickers impression. For all other cases crack lengths were either equal or smaller than the Vickers impression.

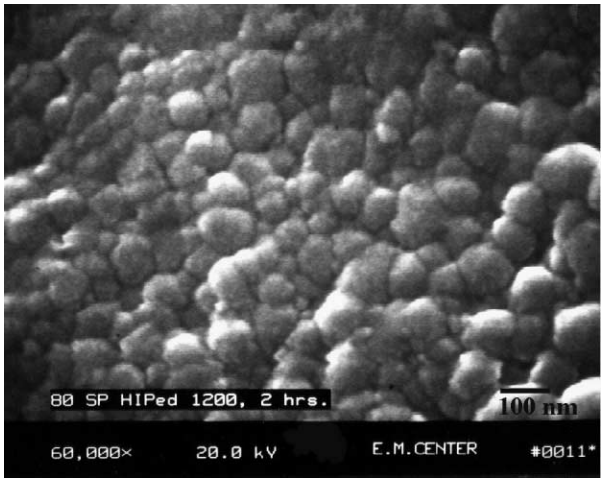

Fig. 2. SEM micrograph of as-etched sample of composition B, HIPed at 1300 °C, 2 h, showing equiaxed nature of the grains, sizes are 100±10 nm.

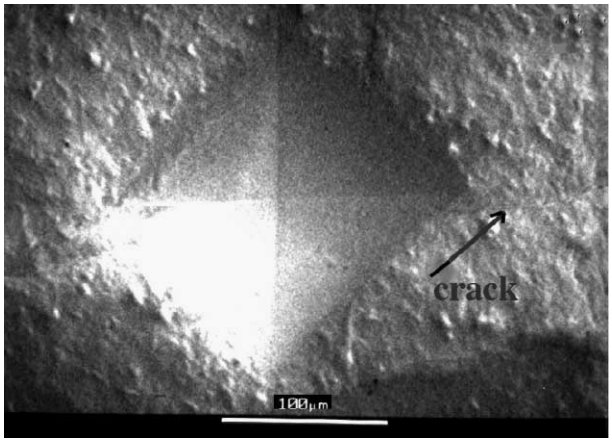

Fig. 3. SEM micrograph of indentation and crack generated by indentation of composition D HIPed at 1200 °C, 2 h.

3.2. Hardness, fracture toughness and hot hardness results

Dense samples of compositions A–D were subjected to indentation tests at room temperature. For the calculation of toughness, the Young's modulus was evaluated using the rule of mixture for composites. Independent evaluation of Young's moduli using a Knoop indenter was not successful because of piling of materials around the corner. For the fracture toughness calculation of composition A, the Niihara et al. [19] equation was used. Whereas, for the other three cases, the Evans and Charles [20] equation was used.

Fig. 4 describes the variation of hardness and fracture toughness of different nano composites. The hardness value was lowest for composition D; for other compositions, the hardness values ranged between 6.03 and 7.79 GPa. The fracture toughness of composition A was 5.31 MPa$\sqrt{m}$, while fracture toughness of other compositions ranged between 2.7 and 2.89 MPa$\sqrt{m}$. So, based on the results, we can conclude that composition A, which has an α-Al_2O_3–$MgAl_2O_4$ nanocomposite structure, had better hardness and fracture toughness values than other compositions. To the best of our knowledge, no such data are available in the literature.

It is important at this point to compare the present results with those in the literature. Typically, the hardness of coarse-grained $MgAl_2O_4$ is about 12.7 GPa. So, reduction of hardness was observed in all compositions compared with the conventional $MgAl_2O_4$. Ghosh et al. [5] reported fracture toughness of about 1.80 MPa$\sqrt{m}$ obtained by both chevron notch and controlled microflow technique. The average grain size was 10–100 μm. Sakai et al. [6] also reported a similar value. These values are in agreement with the controlled microflaw technique obtained by Stewart and Bradt [4] for a pure $MgAl_2O_4$ material. Except for composition A, in the other three compositions, fracture toughness was slightly larger than the reported values. In composition A, fracture toughness was more than double the value; indicating that nano Al_2O_3 plays a significant role in enhancing the fracture toughness presumably restraining the grain growth.

Fig. 5 shows the hot hardness results of composition A. Hardness did not change much up to 1000 °C; beyond that it decreased significantly. The hardness of the composite ($MgAl_2O_4$–Al_2O_3) at 1000 °C was one third of the room temperature hardness. The contribution of dislocation can be ruled out in the present case since dislocation density was negligible as such in the case of nanocrystalline materials. In ceramic materials, diffusional creep is significant only at high temperatures close to the melting point but, for the small grained ceramic materials, significant diffusional creep was achieved at lower temperatures [21,22]. Nevertheless, it may be possible that, above 1000 °C, thermally activated

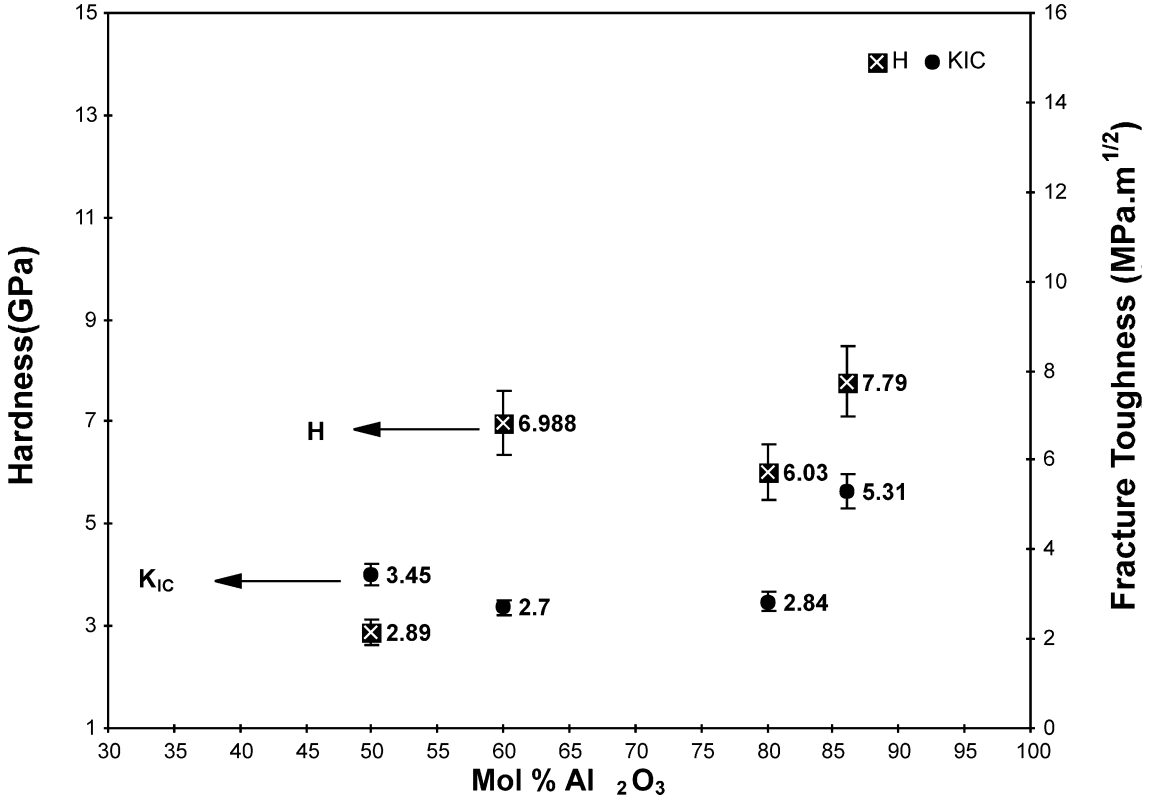

Fig. 4. Hardness, fracture toughness values of different compositions.

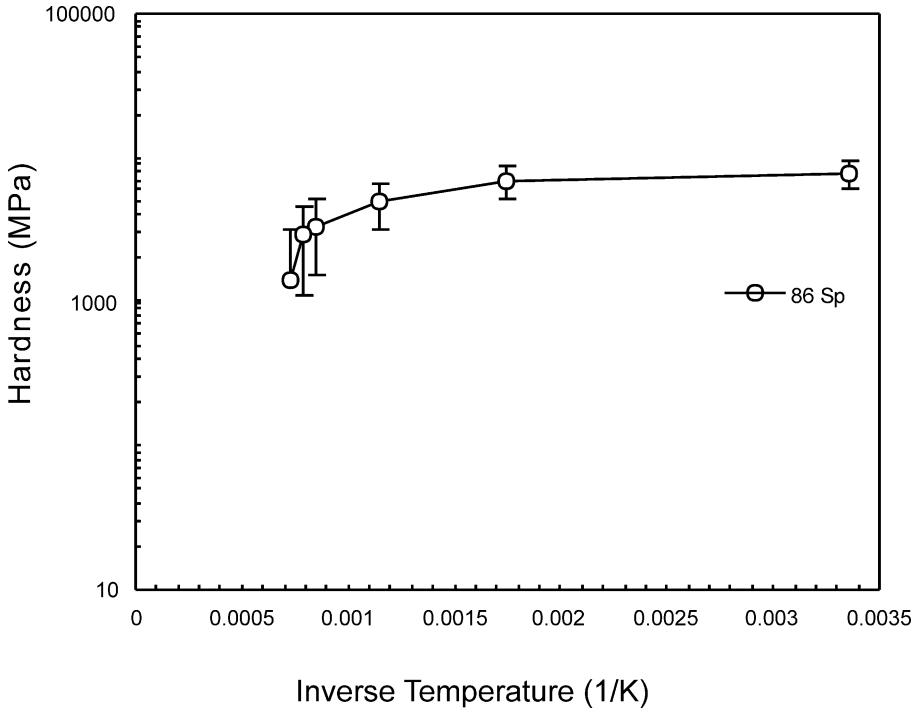

Fig. 5. Hot hardness results of composition A.

deformation was initiated by the diffusional creep process and, hence, the reduction of hardness occurred. Based on the present results, little can be said about which mechanism of creep was predominant. Similar hot hardness experiments were performed by Hahn and Averback [21] for nano TiO_2. For nano TiO_2, hardness reduction occurred at a temperature as low as 430 °C. Wakai et al. [22] reported superplastic elongation larger than 150% at 1600 °C at an initial strain rate of 4.10^{-5} s^{-1} for Si_3N_4–SiC nanocomposites material. It is likely that the retention of nanocrystalline structure is helpful for possible superplastic deformation of spinel and related composites.

4. Conclusions

Both room temperature and high temperature mechanical properties of dense nanocrystalline $MgAl_2O_4$ and its composites were evaluated and compared with the existing literature for coarse grained materials. The hardness values of $MgAl_2O_4$–Al_2O_3 and $MgAl_2O_4$–MgO were between 2.89–7.79 GPa and fracture toughness values were from 2.5–5.82 MPa$\sqrt{m}$. The hardness values of present nanocomposite materials were typically lower than the coarse grained pure $MgAl_2O_4$ and the fracture toughness of one such composite material (Al_2O_3– $MgAl_2O_4$) was more than double the value of the conventional material. Hot hardness results showed that a reduction in hardness occurred at 1000 °C, which may be particularly beneficial for superplastic deformation

Acknowledgements

This work is supported by NSF grant No DMII-9800009.

References

[1] G.E. Fougere, J.R. Weertman, R.W. Siegel, Nanostr. Mater. 5 (1995) 127.
[2] S. Bhaduri, S.B. Bhaduri, J.O.M. 50 (1998) 44.
[3] K. Niihara, J. Ceram. Soc. Japan 99 (1991) 974.
[4] R.L. Stewart, R.C. Bradt, J. Am. Ceram. Soc. 63 (1980) 619.
[5] A. Ghosh, K.W. White, M.G. Jenkins, A.S. Kobayashi, R.C. Bradt, J. Am. Ceram. Soc. 74 (1991) 1624.
[6] M. Sakai, R.C. Bradt, A.S. Kobayashi, Nippon Seramikkusu Kyokai Gakujutsu Ronbunshi 96 (1988) 525.
[7] J.C. Hay, K.W. White, J. Am. Ceram. Soc. 76 (1993) 1849.
[8] K.W. White, G.P. Kelkar, J. Am. Ceram. Soc. 74 (1991) 1732.
[9] G.S. Corman, J. Mater. Sci. Lett. 11 (1992) 1657.
[10] F. Beclin, R. Duclos, J. Crampon, F. Valin, Acta. Metall. 43 (1995) 2753.
[11] R. Lappalainen, A. Pannikkat, R. Raj, Acta. Metall. Mater. 41 (1993) 1229.
[12] D. Duclos, N. Doukhan, B. Escaig, J. Mater. Sci. 13 (1978) 1740.
[13] K.C. Radford, C.W.A. Newey, Proc. Br. Ceram. Soc. 9 (1967) 131.
[14] H.A. Maguire Jr, R.L. Gentilman, Ceram. Bull. 60 (1981) 255.
[15] T.E. Mitchel, L. Hwang, A.H. Heuer, J. Mater. Sci. 11 (1976) 264.
[16] P.C. Panda, R. Raj, P.E.D. Morgan, J. Am. Ceram. Soc. 68 (1985) 522.
[17] S. Bhaduri, S.B. Bhaduri, K.A. Prisbrey, J. Mater. Res. 14 (1999) 3571.
[18] S. Bhaduri, S.B. Bhaduri, Nanostr. Mater. 11 (1999) 469.

[19] A.G. Evans, E.A. Charles, J. Am. Ceram. Soc. 59 (1976) 371.
[20] K. Niihara, R. Morena, D.P.H. Hasselman, J. Mater. Sci. Lett. 1 (1982) 13.
[21] H. Hahn, R.S. Averback, Nanostr. Mater. 1 (1992) 95.
[22] F. Wakai, Y. Kodama, S. Sakaguchi, N. Murayama, K. Izaki, K. Niihara, Mater. Res. Soc. Symp. Proc. 196 (1990) 349.